The added value of CT virtual angioscopy to MDCT angiography in the evaluation of aortic diseases

Mohammad Abd Alkhalik Basha[1] · Ahmed Fekry Salem[1] · Taghreed M. Azmy[1] · Samar Mohamad Shehata[1]

Abstract

Purpose Incorporation of virtual angioscopy (VA) in the diagnostic work-up of aortic diseases could improve the clinical value and efficiency of multidetector computed tomography angiography (MDCTA). We aim to evaluate the clinical usefulness of virtual aortic navigation by CT angiography in various aortic diseases as a complement to standard MDCTA.

Materials and methods We retrospectively selected 211 patients who performed MDCTA for suspected or operated aortic diseases. VA endoluminal images of the aorta were obtained by a fly-through technique. Two senior vascular radiologists independently evaluated all MDCTA images. After 1 month, the same two radiologists independently reviewed the MDCTA images combined with CTVA images. The respective accuracy of CTVA in delineating aortic abnormalities was compared to that of MDCTA using Fisher's exact test. The Fleiss kappa (κ) statistic was used to assess the inter-reader agreement (IRA).

Results We detected 229 abnormalities in 203 patients on MDCTA and 231 abnormalities in 205 patients on CTVA. CTVA provided significant additional findings in 63.8% (146/229) of all abnormalities diagnosed by MDCTA ($p < 0.001$, odd ratio [OR] = 42). Although CTVA diagnosed two abnormalities overlooked by MDCTA, the value was statistically insignificant ($p = 0.787$, OR = 1.3). Regarding postoperative abnormalities, the CTVA added significant additional findings over MDCTA ($p = 0.006$, OR = 87.4). The overall IRA for the performance of CTVA was good ($κ = 0.699$).

Conclusions CTVA yields extra findings and improves diagnostic efficiency of MDCTA, especially in postoperative patients.

Keywords Computed tomography angiography · Virtual angioscopy · Aortic diseases

Introduction

The field of virtual diagnosis has emerged to clinical medicine with the recent advances in computed tomography (CT) and magnetic resonance imaging (MRI) [1, 2]. The

✉ Mohammad Abd Alkhalik Basha
   Mohammad_basha76@yahoo.com

   Ahmed Fekry Salem
   Radahmedfs@hotmail.com

   Taghreed M. Azmy
   taghreedazmy@hotmail.com

   Samar Mohamad Shehata
   samarshehata2003@gmail.com

1 Department of Radio-Diagnosis, Zagazig University, Zagazig, Egypt

non-invasive examination of the cavities within the human body was possible due to significant improvement in image quality and new software for three-dimensional (3D) post-processing [3].

Virtual angioscopy (VA) was first reported in 1996 by Davis et al. [4] using MRI and 2 years later by Smith et al. [5] using CT. CTVA is an image-processing technique that uses datasets from CT angiography to provide endoluminal views of blood vessels [6]. It is similar to a camera inside blood vessels that allows image of internal contour of vasculatures, for which it has been named 'VA' [5]. It is based on the notion of active vision in which only visual perception drives the motion of the virtual angioscope [7]. Compared to multiplanar reformations, CTVA enables a better accurate localization of aortic wall abnormalities and their relation with aortic arch branches. Preliminary studies indicate its promising role for non-invasive assessment of vascular disorders [8].

Due to the recent advancement of high-resolution CT scanners and the development of computer graphics and

software, the application of CTVA is increasing, and its specific uses and challenges in diagnostic medicine are being explored. In this study, we aimed to assess the clinical usefulness of virtual aortic navigation by CT angiography in various aortic diseases as a complement to standard MDCTA.

Materials and methods

Ethical considerations

The institutional review board approved the study, and a waiver of individual patient consent was obtained. The study was conducted according to the ethical rules of declaration of Helsinki.

Study population

We searched our electronic database between January 2016 and December 2018. We found 219 patients who were referred to our institution for MDCTA of the aorta for suspected aortic diseases like aneurysms, traumatic aortic transection, dissection, and follow-up of patients with prior surgical or endovascular procedure. Inclusion criteria were patients with suspected congenital and acquired aortic lesions (pre or postoperative) with good quality images. Exclusion criteria were poor quality images due to motion artifacts or incomplete datasets (8 patients). This yielded a final total number of 211 patients. Flow chart of our study is illustrated in Fig. 1.

MDCTA technique

All images were obtained using 128 detectors row CT scanner (Philips Healthcare- Ingenuity). The image field extended between the carotid bifurcation and the femoral artery. A 120 ml Iohexol (Visipaque, Amersham Health, SA, Velizy, France), with an iodine concentration of 320 mg, was injected intravenously (IV) at a rate of 4–5 ml/s for adult patients. In pediatric patients, non-ionic contrast media (Ultravist/Omnipaque 350) was injected at a dose of 1.5–2 mL/kg through an 18 to 24-gauge intravenous catheter into the right antecubital vein with a flow rate of 3 mL/s using a programmed power injector pump. The start time of imaging was settled in each patient by computer-assisted bolus tracking (Bolus Pro, Ultra; Philips Medical Systems). When an ascending aortic lesion was suspected, a contrast-enhanced retrospective ECG gated scan was obtained to evaluate the aortic root, aortic valve, and coronary arteries. The MDCT protocol was achieved as follows: 0.6 mm reconstruction increment, 0.6 mm collimation width, standard abdominal filter, 40 cm field of view, 0.3 pitch, 0.4 s X-ray
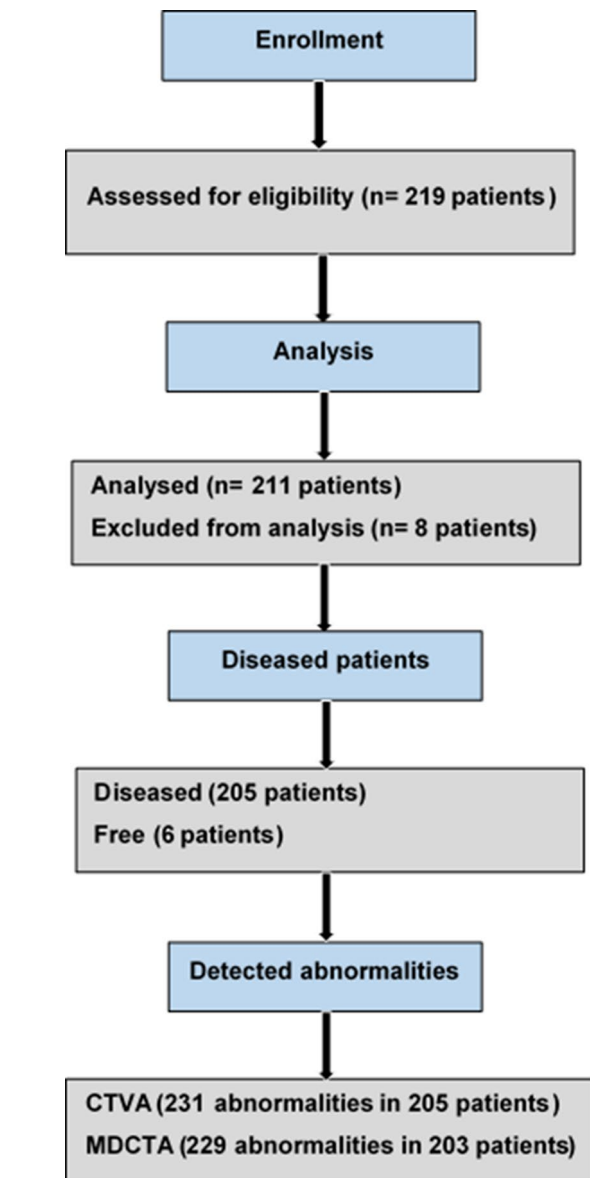
Fig. 1 Flowchart of our study. *MDCTA* multidetector computed tomography angiography, *CTVA* computed tomography virtual angioscopy

tube rotation time, 80–100 kV tube voltage, and 400–700 mAs tube current.

Virtual angioscopy (VA) technique

The VA endoluminal images of the aorta were produced by applying a reverse window-level transfer function using a software program. The vessel centerline was segmented manually using a full mode fly-through navigation for a detailed description and localization of the lesion in relation to major aortic branches and aortic valve. For width (W) and level (L); voxels with Hounsfield (HU) value below $W - l/2$

were completely white and opaque, while voxels with HU value greater than $W + l/2$ were completely black and translucent Voxels with HU value between $W − l/2$ and $W + l/2$ were gray and partially opaque. The W and L were chosen in such a way that contrast-enhanced blood added little contribution to the image. The interface between enhanced vasculature and unenhanced soft tissue was gray and somewhat opaque, enabling clear visualization of the vessel wall. The enhanced blood was dark and translucent so that the luminal contents and surface of the vessel were not obscured. The surrounding soft tissues were bright and opaque, which obscured visualization of the vessel lumen. By applying a clip plane (a simple, yet interactive editing technique used to remove slabs of data), the surrounding soft tissues were removed to visualize the vessel lumen. Effectively, the clip opened a window into the vessel interior so that the vascular lumen was displayed. Alternatively, a fly-through technique was used to visualize the vessel lumen and its contents. The mean time to reconstruct and interpret 3D endoluminal aortic view images was $6.7 ± 2.1$ min. Movies 1 and 2 in Electronic Supplementary Material describe the fly-through technique in real-time.

Image analysis and interpretation

Image datasets were reconstructed with 0.6/1.25 mm slice thickness and analyzed on a dedicated platform Extended Brilliance Workstation (Philips Medical System, Best, The Netherlands). For each patient, multiplanar reformation (MPR), maximum intensity projections (MIPs), and 3D display volume-rendering (VR) images were reconstructed. Additionally, sagittal and coronal oblique MPR images were obtained to compensate for aortic arch curvature. CTVA reconstruction was done in all patients. We manually performed navigation mode with the VR thresholds, and spatial rendering created endoluminal views. Full fly-through navigation mode with 3D reconstructions of the aortic wall was used in all patients. Empty fly-through navigation mode after aortic wall subtraction was used only in patients treated with endovascular aortic repair (EVAR) to analyze stent-graft components.

Two senior vascular radiologists with over 10 years of experience in vascular imaging, independently evaluated all MDCTA images alone. After 1 month, the same two radiologists independently reviewed the MDCTA images combined with CTVA images to diminish the memory bias of readers. Any discrepancies in interpretation were resolved by a third senior vascular radiologist with over 15 years of experience in vascular imaging. All radiologists were blinded to any clinical information, but they assessed the following items: Congenital aortic abnormalities, calcifications, ulcerated plaques, stenosis, clot or thrombus, aneurysms, dissections, size, configuration, and location of intimal tears/

fenestrations, side branches, and restenosis after vascular stenting or endovascular aortic repair.

Statistical analysis

The collected data were computerized and statistically analyzed using MedCalc 13 (MedCalc Software bvba, Ostend, Belgium). Quantitative variables were presented as mean ± standard deviation (SD), and categorical variables were presented as number and percentage. The Fleiss kappa (κ) statistic and 95% confidence intervals (CIs) were used to assess the inter-reader agreement (IRA) of evaluated items by MDCTA and CTVA. The κ values were interpreted as follows: poor agreement = 0.01–0.20; fair agreement = 0.21–0.40; moderate agreement = 0.41–0.60; good agreement = 0.61–0.80; and very good agreement = 0.81–1.0. The odd ratio (OR) with 95% CI was calculated. Fisher's exact test was used to assess the statistically significant difference between CTVA and MDCTA as regard respective accuracy. A $p < 0.05$ was considered statistically significant.

Results

Patients

This retrospective study reviewed 211 patients with suspected aortic diseases throughout the 3 year study period. The mean age was $49 ± 11.5$ years, the range was 7 days to 75 years, 114 (54%) patients were males, and 97 (46%) were females. The patients' data are summarized in Table 1. All MDCTA scans with 3D datasets and CTVA were obtained in all patients with high-quality images. We detected 229 aortic abnormalities with MDCTA in 203 patients and 231 aortic abnormalities with combined CTVA and MDCTA in 205 patients (Table 2).

Table 1 Patients' data and cardiovascular risk factors

Characteristics	No (%)
Age (years) (Mean ± SD)	49 ± 11.5
Male: Female	114/97
Smoking	131 (62.1)
Hypertension	63 (29.9)
Dyslipidemia	119 (56.4)
Diabetes mellitus	111 (52.6)
Family history	95 (45)

Unless otherwise indicated, data are number and percentage in parenthesis

SD standard deviation

Table 2 Aortic abnormalities detected in 211 patients

Abnormalities	No (%)
Atherosclerosis ± partial thrombosis	81 (35)
Aortic aneurysms	53 (22.9)
Aortic dissections	34 (14.7)
Aortic coarctation	18 (7.8)
Postoperative	11 (4.8)
Tubular hypoplasia of aortic arch	8 (3.5)
Double aortic arch	7 (3)
Le rich syndrome	7 (3)
Interrupted aortic arch	5 (2.2)
Truncus arteriosus	4 (1.7)
Type V Takayasu arteritis	2 (0.9)
Tausig Bing anomaly	1 (0.4)
Total	231 (100)

Data are number and percentage in parenthesis

Image findings

CTVA demonstrated the distribution of atherosclerotic plaques on the aortic wall as irregular surfaces with floating calcification in 64/81 (79%) of abnormalities, and accurately detected the relation to the nearby branches' ostia. In contrast, 8/17 (47.1%) of abnormalities with non-calcified soft plaques and without significant luminal narrowing were poorly visualized on CTVA and hence interpreted as vessel wall alterations (Fig. 2). In 53 abnormalities with aortic aneurysms, CTVA diagnosed a case of intimal tear within an unstable aortic arch aneurysm that was not seen in conventional MDCTA (Fig. 3). In 34 abnormalities with aortic dissections, the locations, types, true and false lumens, as well as the fenestrations sites in dissection flaps were depicted by CTVA (Fig. 4). In all abnormalities with coarctations (n = 18), the degree of vessel narrowing is visually estimated

from the inside on CTVA and readily correlated with the degree measured on MDCTA images. In all patients who underwent surgical or interventional procedures (n = 11), estimation of the exact size of the stent lumen was inaccurate on MDCTA in 81.8% (9/11) of patients due to stent artifact. However, the fly-through technique was accurately performed along the examined stents (Fig. 5).

The added diagnostic value

CTVA detected two aortic abnormalities missed by MDCTA, one with intimal tear within an unstable aortic arch aneurysm. The other was in-stent restenosis and poor apposition of the proximal rim of the stent in relation to the wall of the aorta. In all abnormalities diagnosed by MDCTA, all radiologists accepted that CTVA produced additional findings in 63.8% (146/229) of lesions (Table 3). Regarding postoperative abnormalities, the CTVA provided additional findings over MDCTA in 81.8% (9/11) of lesions. In congenital abnormalities, all radiologists accepted that MDCTA was superior to CTVA in 26.8% (11/41) of lesions.

The respective accuracy of MDCTA and CTVA in delineating aortic abnormalities in 211 examined patients was compared (Table 4). Although CTVA diagnosed an abnormality not identified by MDCTA in two patients, the value was not statistically significant, based on Fisher's test ($p = 0.588$, OR 1.3, 95% CI 0.459–3.95). The rate of additional findings produced by CTVA was statistically significant ($p < 0.001$, OR 42, 95% CI 18.3–96.6). Regarding postoperative abnormalities, the CTVA provided significant additional findings over MDCTA ($p = 0.006$, OR 87.4, 95% CI 3.7–2051.2). Regarding congenital abnormalities, the CTVA did not add significant additional findings over MDCT. Even though, the MDCTA provided a statistically significant additional findings over CTVA (p 0.02, OR 0.034, 95% CI 0.002–0.6).

Fig. 2 A 57-year-old woman with a non-calcified plaque. **a** Sagittal MDCTA image shows soft tissue plaque protrudes into the lumen of descending aorta, extends into the celiac trunk, and exerts luminal narrowing (arrow). **b** CTVA image shows vessel wall alteration by a structure with a density close to the vessel wall, protrudes within the lumen, and exerts luminal narrowing (arrow)
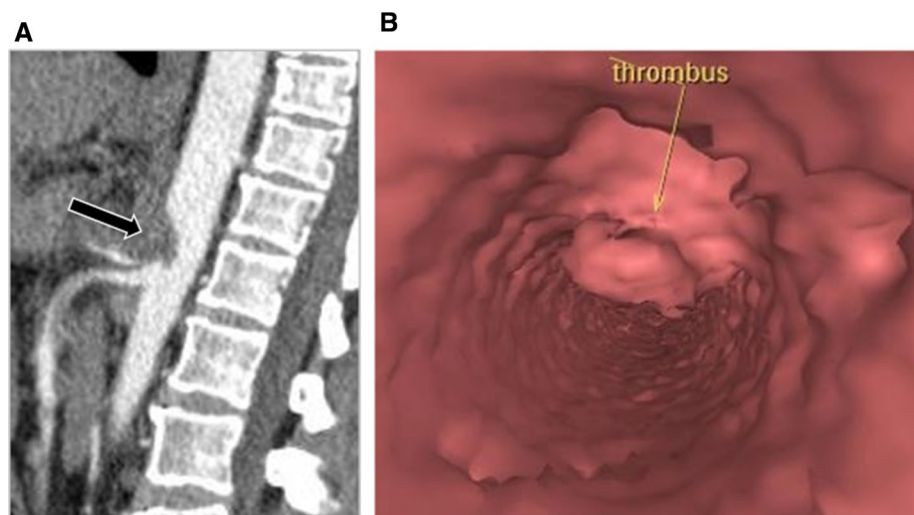
Fig. 3 A 46-year-old man with a ruptured aortic arch aneurysm. **a** and **b** Coronal MDCTA images show signs of aneurysmal rupture/instability as hyperdensity within the aneurysm, and mild hemomediastinum indenting the right pulmonary artery (arrows). **c** and **d** CTVA images reveal the irregular outline of the aortic arch and the brachiocephalic trunk by the contained hematoma that compresses the wall and encroaches upon the lumen (arrows in c). Also, CTVA shows an intimal tear at the level of brachiocephalic trunk not seen in MDCTA (arrow in d)
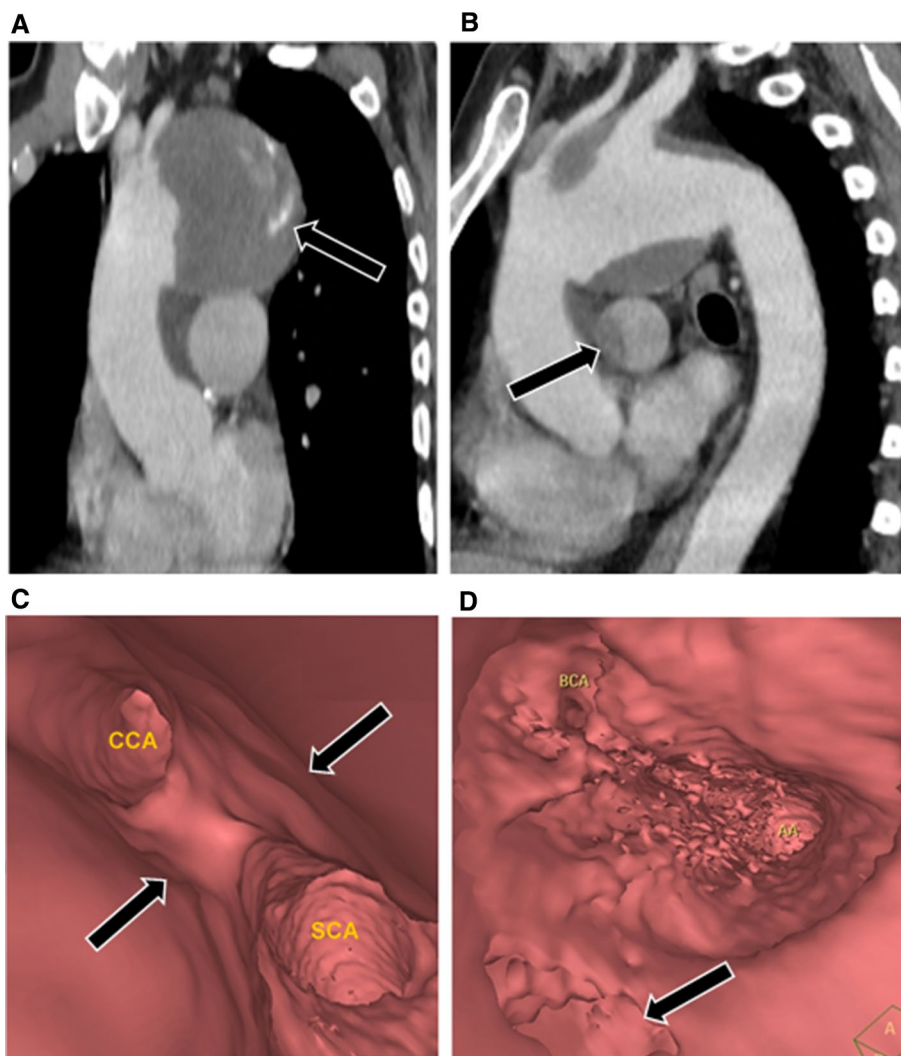
Inter-reader agreement (IRA)

The IRA was moderate to very good regarding the evaluated items by MDCTA ($\kappa = 0.451$–0.873), and fair to very good regarding the items being assessed by CTVA ($\kappa = 0.360$–0.877). The IRA was good regarding the overall diagnosis for MDCTA and CTVA ($\kappa = 0.744$ and 0.699, respectively) (Table 5).

Discussion

Recently, many improvements have been made in vascular imaging for better evaluation of aortic diseases. Although CTVA has been described since 1996 [4], the uses of CTVA in aortic diseases are mainly limited to research purposes in most published reports in the literature. However, some literature suggested that CTVA could add extra benefits in comparison to MDCTA [9–11]. In the current study, we

wondered if the addition of CTVA improves the diagnostic accuracy of MDCTA in the assessment of various aortic diseases. To reach this goal, we retrospectively evaluated MDCTA and virtual angioscopic examinations of 211 patients with suspected or operated aortic diseases. We found that CTVA detected two aortic abnormalities missed by MDCTA and provided additional findings in 63.8% of aortic abnormalities. Our preliminary experiences are congruent with those mentioned in previous studies [11–14] and recommend the addition of CTVA to MDCTA protocol in the evaluation of aortic diseases.

Although CTVA demonstrated the distribution of atherosclerotic plaques on the aortic wall in 64/81 (79%) of our aortic abnormalities, conventional MDCTA, MIPs and MPR were superior to CTVA in localization and characterization of soft non-calcified plaques. This finding resembles that mentioned by Carrascosa et al. [15].

Various studies have suggested that MDCTA is the imaging modality of choice for the pre- and postoperative

Fig. 4 A 63-year-old man with Stanford A aortic dissection. **a** Sagittal MDCTA image shows irregularly shaped dissecting flap (arrow) extends from the aortic root through the aortic arch down to descending aorta with total thrombosis of false lumen (FL). **b** Axial MDCTA image shows the flap (arrow) extending into the brachiocephalic trunk with the patently true lumen. **c** CTVA shows irregular endoluminal surface and luminal indentation by a thrombosed false lumen (arrows). **d** CTVA shows sheet-like intimal flap separating true from the false lumen (arrows)
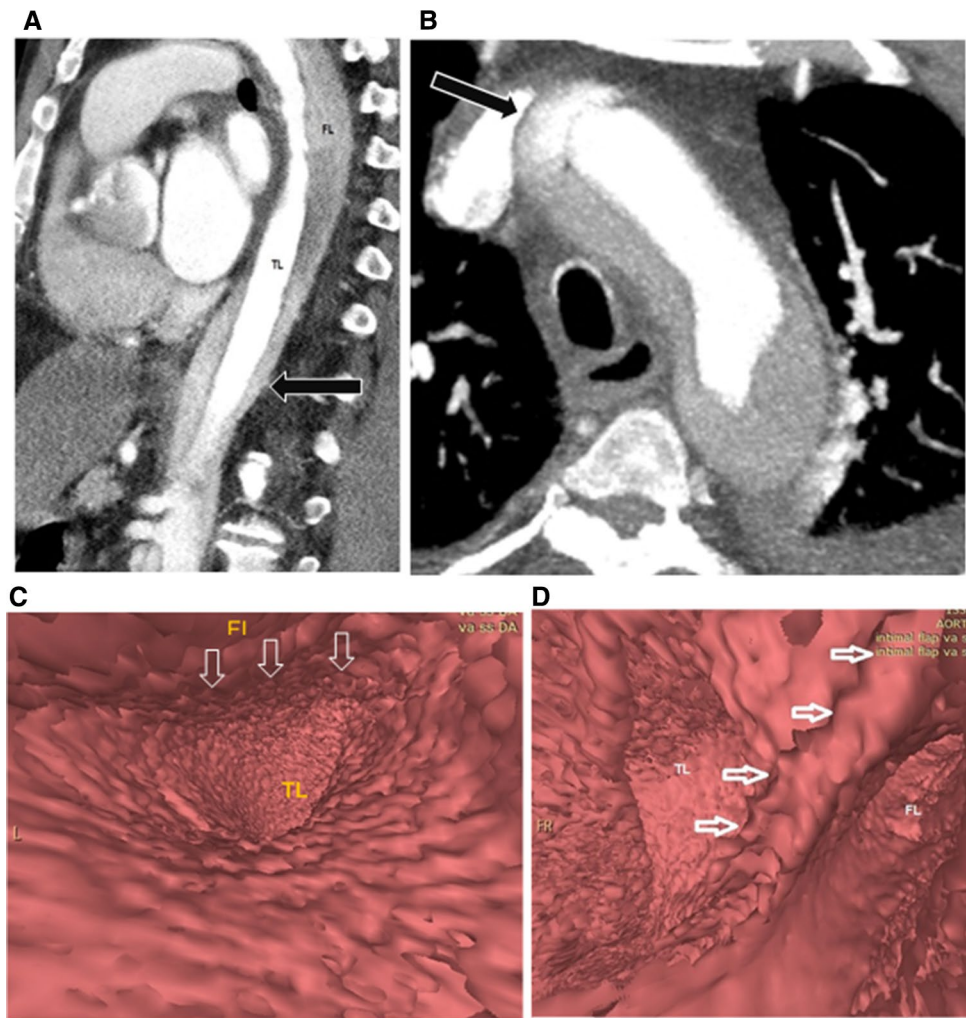

evaluation of abdominal aortic aneurysms [15–19]. In our study, CTVA demonstrated the volume and shape of all aneurysms and estimated neck size and its relation to the major aortic branches in all patients. CTVA showed the parent blood vessels, aneurysmal lumen calcification, and thrombosis. It determined the relation of the aneurysm to the ostia of aortic branches on the inner surface of the aneurysm wall. Also, CTVA detected the site, shape, size, and extension of an intimal tear within an unstable aortic arch aneurysm that was not seen in MDCTA.

Preoperative determination of the extent of aortic dissection in relation to the arterial branches is very essential. Recently, MDCTA has provided a high diagnostic accuracy for the evaluation of aortic dissection [20–22]. The extension of dissection to the major aortic branches that originated off the true or false lumen was visible on CTVA in all patients with dissection in our study. Additionally, CTVA enabled correct visualization and detailed characterization of the intimal flap and the sites of entry and reentry tears in all patients with aortic dissection. CTVA allowed the understanding of the relationship between the false lumen and major aortic branches, which must be taken into consideration when planning for surgical or endovascular procedures. A correlation with 2D axial, MIP, MPR, and 2D VR images allowed a better interpretation of the CTVA views. These findings are similar to those reported in previous studies [6, 23].

In our study, we had one patient with intimal tear within an unstable aortic arch aneurysm. Though MDCTA did not clearly show the intimal tear in a general view, CTVA provided the exact size and location of the tear preoperatively. CTVA is very valuable for discriminating intramural hematoma from a thrombosed-type acute aortic dissection, which may facilitate therapeutic planning.

In line with previous studies [11, 24–28], our study showed that CTVA provided a major potential role in the assessment of stent-graft in postoperative patients. It accurately estimated the gap between the proximal rim of stent-graft in relation to the aortic wall and the ostia of major aortic branches. It illustrated the morphological details of the internal stent wires, lining, and the vessel endothelium. Moreover, we found that the estimation of the exact size of the stent lumen on MDCTA was limited by stent artifact
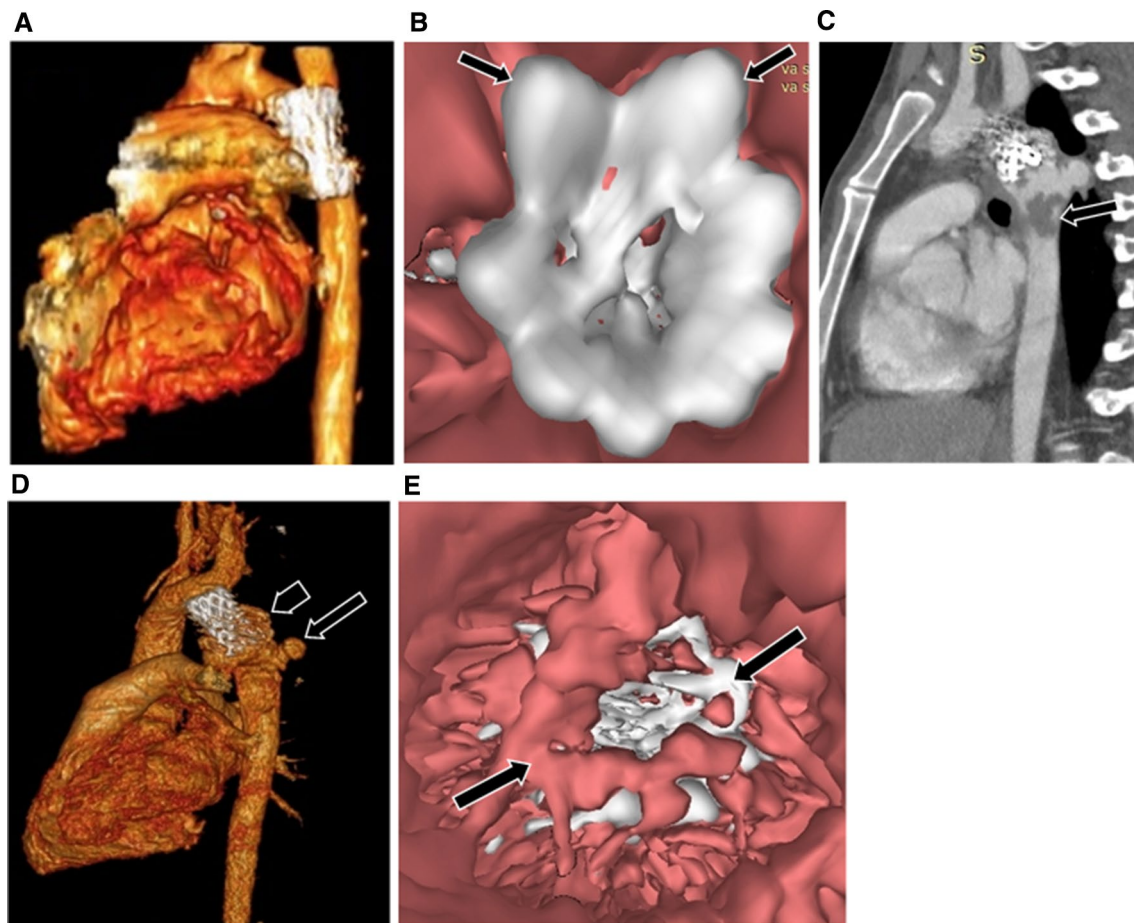
Fig. 5 A 26-year-old man with stenting of native coarctation. **a** VR image shows the proper positioning of the stent with adequate dilatation of the coarctation segment. **b** CTVA image demonstrates with high details the stent patency with poor apposition of the proximal rim of the stent in relation to the aortic wall (arrows). **c** MIP and **d** VR Follow up images 1 year later reveal soft tissue plaque within descending aorta (arrow in c), endoleak (arrowhead in d), and aneurysmal dilatation involving the distal stent with a smaller posterior secular aneurysm (arrow in d). **e** Follow up CTVA image shows in-stent restenosis (white arrow) and soft tissue thrombus (black arrow) covering the stent struts

Table 3 Distribution of extra findings identified in 146 aortic abnormalities by CTVA

Abnormalities	No. of findings
Atherosclerosis	64 (43.8)
Aortic aneurysms	44 (30.1)
Aortic dissections	27 (18.5)
Aortic coarctation	2 (1.4)
Postoperative	9 (6.2)
Total	146 (100)

Data are number and percentage in parenthesis

CTVA computed tomography virtual angioscopy

in nine patients. However, the fly-through technique was accurately performed along all examined stents. In a study conducted by Louis et al. [11] on 103 patients undergoing EVAR of aortic dissection and aortic aneurysm, they reported that CTVA provided additional data compared to MDCTA in > 76% of patients.

Interestingly, regarding the congenital abnormalities, the CTVA did not add significant value over MDCTA. Moreover, the MDCTA provided statistically significant additional findings over CTVA regarding the 3D-delineation of the aortic anomalies as well as associated cardiac and coronary artery anomalies.

In the current study, the overall agreement between readers for the performance of CTVA was good. This may be explained by the higher experience of readers and the exclusion of bad quality images. However, this may contribute to bias and potentially affecting the diagnostic performance of CTVA.

Finally, we believe that the role of CTVA in various aortic diseases still requires to be established. However, in

Table 4 Comparison between MDCTA and CTVA as regard respective accuracy in delineating aortic abnormalities

	Missed abnormalities By MDCTA	Overall additional findings By CTVA over NDCT	Additional findings by CTVA in Postoperative abnormalities	Additional findings by MDCTA in Congenital abnormalities
No	2/211	146/229	9/11	11/41
OR	1.3465	42.0306	87.4000	0.03437
95% CI	0.459–3.9497	18.2907–96.5829	3.7241–2051.1751	0.001967–0.6005
z statistic	0.542	8.807	3.7241 to 2051.1751	2.309
P-value	0.5880	<0.0001	0.0055	0.0209

MDCTA multidetector computed tomography angiography, *CTVA* computed tomography virtual angioscopy, *OR* odd ratio, *CI* confidence interval

Table 5 Inter-reader agreement of evaluated items by MDCTA or CTVA

Items	MDCTA		CTVA	
	κ coefficients	95% CI	κ coefficients	95% CI
Congenital aortic abnormalities	0.756	0.634 to 0.878	0.360	0.0846 to 0.636
Calcifications	0.873	0.751 to 0.996	0.691	0.560 to 0.822
Ulcerated plaques	0.494	0.241 to 0.746	0.505	0.291 to 0.720
Stenosis	0.759	0.618 to 0.900	0.808	0.663 to 0.952
Clot or thrombus	0.706	0.512 to 0.900	0.512	0.257 to 0.767
Aneurysms	0.773	0.572 to 0.973	0.605	0.332 to 0.879
Dissections	0.831	0.660 to 1.000	0.808	0.658 to 0.957
Intimal tears/fenestrations	0.485	0.214 to 0.756	0.877	0.727 to 1.000
Side branches	0.639	0.372 to 0.906	0.817	0.636 to 0.999
Restenosis after operation	0.451	0.0942 to 0.808	0.765	0.622 to 0.908
Overall diagnosis	0.744	0.528 to 0.959	0.699	0.498 to 0.899

MDCTA multidetector computed tomography angiography, *CTVA* computed tomography virtual, *CI* confidence interval

particular patients, specifically, postoperative patients, the application of CTVA enhances the diagnostic confidence and aid decision making with which endovascular re-intervention is performed. Nevertheless, the use of this imaging technique needs experiences, adequate caseload, and time since it is based on precise gating for image reliability. Moreover, the cost burden of using CTVA is another limitation of this technique. Thus the use of CTVA should be restricted to suspected cases when there is still doubt in the diagnosis after performing MDCTA.

The current study had some limitations. First, the study was conducted at a single center. Second, the study was performed retrospectively with a high possibility of bias. Third, the motion, the surgical clips in bypass, and the metallic artifacts can be readily recognized on the 3D view; however, it may be misinterpreted as apparent stenosis on the fly-through technique. Fourth, the cost-effectiveness of using CTVA may be a drawback of this technique. Fifth, all images were analyzed by highly experienced radiologists; this is potentially affecting the diagnostic performance of CTVA and explain the good inter-reader agreement in our study. Thus, further studies about the performance of this technique when applied by less experienced radiologists are needed. Sixth, there were no enough pediatric patients in our study to predict the validity of CTVA in this age group. Finally, absence of a reference standard to validate the results of the fly-through technique.

In conclusion, the addition of CTVA increased the diagnostic accuracy of MDCTA for the evaluation of aortic diseases, especially in postoperative patients. Therefore, CTVA should be included during work-up for those patients. Future prospective studies with a large sample size should be performed to assess the diagnostic performance of CTVA and validate it with a strong gold standard where appropriate. Also to determine how CTVA findings will influence patient care and monitor interventions in patients with various aortic diseases.

Compliance with ethical standards

Conflict of interest The authors of this manuscript declare no relevant conflicts of interest, and no relationships with any companies, whose products or services may be related to the subject matter of the article.

Ethical approval Institutional review board approval was obtained.

Informed consent Written informed consent was waived.

References

1. Schroeder S, Kopp AF, Ohnesorge B, Loke-Gie H, Kuettner A, Baumbach A, et al. Virtual coronary angioscopy using multislice computed tomography. Heart 2002; 87: 205-209.
2. Fletcher JG, Luboldt W. CT colonography and MR colonography: current status, research directions and comparison. European radiology 2000; 10:786-801.
3. Potchen EJ. Prospects for progress in diagnostic imaging. Journal of internal medicine 2001; 249: 95-108.
4. Davis CP, Ladd ME, Romanowski BJ, Wildermuth S, Knoplioch JF, Debatin JF. Human aorta: preliminary results with virtual endoscopy based on three-dimensional MR imaging data sets. Radiology 1996; 199: 37-40.
5. Smith PA, Heath DG, Fishman EK. Technical Report. Virtual Angioscopy Using Spiral CT and Real-Time Interactive Volume-Rendering Techniques. Journal of computer assisted tomography 1998; 22: 212–214.
6. Maldjian PD, Partyka L. Intimal tears in thoracic aortic dissection: appearance on MDCT with virtual angioscopy. American Journal of Roentgenology 2012; 198: 955-961.
7. Haigron P, Bellemare ME, Acosta O, Goksu C, Kulik C, Rioual K, et al. Depth-map-based scene analysis for active navigation in virtual angioscopy. IEEE Transactions on Medical Imaging 2004; 23: 1380-1390.
8. Louis N, Desgranges P, Kobeiter H, Kirsch M, Becquemin JP. Virtual angioscopy and 3-dimensional navigation findings of the aortic arch after vascular surgery. Circulation 2009; 119: 1052-1055.
9. Izquierdo L, Leiva L. Virtual angioscopy assessment for acute type B aortic dissection endovascular repair. Catheterization and Cardiovascular Interventions 2010; 75: 32-34.
10. Sun Z, Mwipatayi BP, Allen YB, Hartley DE, Lawrence-Brown MM. Computed tomography virtual intravascular endoscopy in the evaluation of fenestrated stent graft repair of abdominal aortic aneurysms. ANZ journal of surgery 2009; 79: 836-840.
11. Louis N, Bruguiere E, Kobeiter H, Desgranges P, Allaire E, Kirsch M, et al. Virtual angioscopy and 3D navigation: a new technique for analysis of the aortic arch after vascular surgery. European Journal of Vascular and Endovascular Surgery 2010; 40: 340-347.
12. Tomás AC, Santos ÁL, Fragata J. Virtual angioscopy and 3D navigation of the aorta. Journal of cardiac surgery 2017; 32: 33-37.
13. Bates WB, Franco A, Keshavamurthy JH. Application of computed tomographic virtual vascular intraluminal endoscopy. The international journal of cardiovascular imaging 2016; 32: 1461-1462.
14. Urbanik A, Chrzan R, Wojciechowski W, Popiela TJ. Virtual angioscopy as an additional feature of angio-CT. InCARS 2003 (p. 1322).
15. Carrascosa P, Capunay C, Vembar M, Ciancibello L, Carrascosa J. Multislice CT virtual angioscopy of the abdomen. Abdominal imaging 2005; 30: 249-258.
16. Nijhof WH, Baltussen EJ, Kant IM, Jager GJ, Slump CH, Rutten MJ. Low-dose CT angiography of the abdominal aorta and reduced contrast medium volume: assessment of image quality and radiation dose. Clinical radiology 2016; 71: 64-73.
17. Diehm N, Herrmann P, Dinkel HP. Multidetector CT angiography versus digital subtraction angiography for aortoiliac length measurements prior to endovascular AAA repair. Journal of Endovascular Therapy 2004; 11: 527-534.
18. Rydberg J, Kopecky KK, Lalka SG, Johnson MS, Dalsing MC, Persohn SA. Stent grafting of abdominal aortic aneurysms: pre- and postoperative evaluation with multislice helical CT. Journal of computer assisted tomography 2001; 25: 580-586.
19. Rydberg J, Kopecky KK, Johnson MS, Patel NH, Persohn SA, Lalka SG. Endovascular repair of abdominal aortic aneurysms: assessment with multislice CT. American Journal of Roentgenology 2001; 177: 607-614.
20. Sun Z, Cao Y. Multislice CT virtual intravascular endoscopy of aortic dissection: a pictorial essay. World J Radiol 2010; 2: 440–448.
21. Sommer WH, Clevert DA, Bamberg F, Helck A, Albrecht E, Reiser MF, et al. Time-resolved computed tomography imaging of the aorta: a feasibility study. Journal of thoracic imaging 2010; 25:161-167.
22. Meinel FG, Nikolaou K, Weidenhagen R, Hellbach K, Helck A, Bamberg F, et al. Time-resolved CT angiography in aortic dissection. European journal of radiology 2012; 81: 3254-3261.
23. Hornero F, Cervera V, Estornell J, Rodriguez I, Buendía JA, Esteban JM, et al. Virtual vascular endoscopy for acute aortic dissection. The Annals of thoracic surgery 2005; 80: 708-710.
24. Sun Z, Winder J, Kelly B, Ellis P, Hirst D. CT virtual intravascular endoscopy of abdominal aortic aneurysms treated with suprarenal endovascular stent grafting. Abdom Imaging 2003; 28: 580–587.
25. Sun Z, Winder RJ, Kelly BE, Ellis PK, Kennedy PT, Hirst DG. Diagnostic value of CT virtual intravascular endoscopy in aortic stent grafting.J Endovasc Ther 2004; 11: 13–15.
26. Sun Z, Allen Y, Nadkarni S, Wright R, Hartley D, Lawrence-Brown M. CT virtual intravascular endoscopy in the visualization of fenestrated endovascular grafts. J Endovasc Ther 2008; 15: 42–51.
27. Sun Z, Chaichana T. Fenestrated stent graft repair of abdominal aortic aneurysm: hemodynamic analysis of effect of fenestrated stents on renal arteries. Korean J Radiol 2010; 11: 95–106.
28. Sun Z, Mwipatayi BP, Semmens JB, Lawrence-Brown MM. Short to midterm outcomes of fenestrated endovascular grafts in the treatment of abdominal aortic aneurysms: a systematic review. J Endovasc Ther 2006; 13: 747–753.

Publisher's Note Springer Nature remains neutral with regard to jurisdictional claims in published maps and institutional affiliations.